

Logarithmic decay in a two-component model

Matthias Sperl

Physik-Department, Technische Universität München, 85747 Garching, Germany

Abstract. The correlation functions near higher-order glass-transition singularities are discussed for a schematic two-component model within the mode-coupling theory for ideal glass-transitions. The correlators decay in leading order like $-\ln(t/\tau)$ and the leading correction introduces characteristic convex and concave patterns in the decay curves. The time scale τ follows a Vogel-Fulcher type law close to the higher-order singularities.

INTRODUCTION

Mode-coupling theory for ideal glass-transitions (MCT) describes the transition from a liquid to a glass as a bifurcation in the equation for the long-time limit of the density-autocorrelation function $\phi_q(t) = \langle \rho_q^*(t) \rho_q \rangle / \langle |\rho_q|^2 \rangle$ for density fluctuations of wave-number modulus $q = |\vec{q}|$. If the long-time limit $f_q = \lim_{t \rightarrow \infty} \phi_q(t)$ reaches zero, $f_q = 0$, the system is in the liquid state. For $f_q > 0$, the system is in a glass state [1]. The theory has been worked out in detail for the hard-sphere system (HSS) [1, 2] where the results of experiments [3] and computer simulations [4] support the validity of MCT. In addition to liquid-glass transitions, MCT also allows for bifurcations of higher order [5]. It can be shown that only bifurcations of a certain hierarchy A_ℓ can arise from MCT [6] which are equivalent to the singularities in the real roots of polynomials of order ℓ upon variation of parameters [7]. The simplest singularity A_2 or *fold* generically occurs when only a single control parameter is changed and the liquid-glass transition is identified with this bifurcation. At the critical value of the control parameter the long-time limit f_q jumps from zero to f_q^c . Close to the singularity and for small $|\phi_q(t) - f_q|$, the correlation functions can be expanded in asymptotic series yielding power laws. A detailed analysis including leading and next-to-leading order results was given for the HSS [2, 8, 9].

An A_3 -singularity or *cusp* can appear when two control parameters are varied. The A_3 -singularity is the end-point of a line of A_2 -singularities which are identified as glass-glass-transition points where a first glass state, characterized by $f_q^1 > 0$, transforms discontinuously into a second glass state with $f_q^c > f_q^1$. At the A_3 , this discontinuity vanishes and the glass-glass-transition line ends. Such cusp was predicted for particles interacting with a hard core and a short-ranged attraction [10, 11] where

density and strength of the attraction are the control parameters. The glass-glass transition takes place between a state dominated by repulsion as in the HSS and a state dominated by attraction, the latter arrested state was proposed to be related to a gel [11].

Tuning a third control-parameter, the extension of the glass-glass-transition line can be varied and once the latter vanishes, the A_3 -singularity merges with the liquid-glass-transition line and gives birth to a *swallowtail* or A_4 -singularity. If the range of the attraction is of the order of 5% of the hard-core diameter such singularity is predicted for a square-well system with a strength of the attraction of several $k_B T$ and a density which is slightly larger than the one for the glassy arrest in the HSS [12].

In contrast to the power-laws at the A_2 -singularity, the dynamics close to higher-order singularities is ruled by the logarithm of the time [5]. The wave-vector dependent asymptotic solutions along with the corrections have been calculated in full generality [13]. The asymptotic laws were demonstrated for the A_3 -singularity of a two-component model [13], and for the higher-order singularities of microscopic models with short-ranged attraction [14]. Logarithmic decays compatible with the predicted scenarios were found in recent computer simulation studies [15, 16].

In the vicinity of an A_3 -singularity, different liquid-glass-transition lines cross, and the dynamics in the liquid regime close to this crossing is influenced by three different singularities. Dynamical scenarios predicted by theory in that region [10, 12, 17] were found in experiments [18, 19, 20, 21, 22, 23] and computer-simulation studies [19, 24]. These findings indicate that such rich dynamics is indeed relevant for these colloidal systems and that asymptotic expansions at the MCT-singularities can interpret the scenario qualitatively and explain the data even quantitatively [17].

In the following, the two-component schematic model

used already in Ref. [13] shall be reconsidered with respect to the A_4 -singularity and the evolution of the time scales. The advantage of the schematic model is that all transition points can be calculated analytically. Even in this simple model typical features of the full microscopic theory are identified. First, the asymptotic laws for the higher-order singularities and the schematic model shall be introduced briefly, further details are found in Ref. [13]. Second, the asymptotic approximation is shown to work well for the correlation functions at the A_4 -singularity. Third, the time scales for the logarithmic decays at A_3 - and A_4 -singularity are discussed for specific paths in control-parameter space.

ASYMPTOTIC LAWS

The A_2 -singularities are characterized by a two-step relaxation around a plateau value, and the asymptotic decay laws are given by scaling functions [2]. For short times the decay onto the plateau is given by a critical decay $\phi_q(t) - f_q(t) = h_q(t_0/t)^a$, while for long times one gets the von Schweidler law $\phi_q(t) - f_q(t) = -h_q(t/t'_\sigma)^b$. The exponents are determined by a single exponent parameter $\lambda = \Gamma(1-a)^2/\Gamma(1-2a) = \Gamma(1+b)^2/\Gamma(1+2b) < 1$. For $\lambda = 1$, the asymptotic solution by power laws becomes invalid and a higher-order singularity occurs. The dynamics at higher-order singularities A_l , $l > 2$ is described up to next-to-leading order by [13]

$$\begin{aligned} \phi_q(t) = (f_q^c + \hat{f}_q) + h_q[(-B + B_1)\ln(t/\tau) \\ + (B_2 + K_q B^2)\ln^2(t/\tau) \\ + B_3 \ln^3(t/\tau) + B_4 \ln^4(t/\tau)] . \end{aligned} \quad (1)$$

The wave-vector-dependent numbers f_q^c , h_q , and K_q are characteristic for a specific singularity, while B , B_i , and \hat{f}_q are in addition functions of the separation parameters ε_1 and ε_2 quantifying the distance of the actual state from the higher-order singularity [13]. The leading order in Eq. (1) is given by the first line with $B_1 = \hat{f}_q = 0$ and the leading order prefactor for the logarithm is $B \propto \sqrt{|\varepsilon_1|}$. The time scale τ is fixed by matching the asymptotic approximation with the numerical solution for $\phi_q(t)$ at the plateau $(f_q^c + \hat{f}_q)$.

THE MODEL

To mimic the q -dependence, which is an important feature of the asymptotic expansions above, we use a two-component model that was introduced for the description of a symmetric molten salt [25]. The model has three control parameters which are combined to the vector $\mathbf{V} = (v_1, v_2, v_3)$. We will use Brownian dynamics, so the

equations of motion for the correlators $\phi_q(t)$, $q = 1, 2$, read

$$\tau_q \partial_t \phi_q(t) + \phi_q(t) + \int_0^t m_q(t-t') \partial_{t'} \phi_q(t') dt' = 0, \quad (2a)$$

$$m_1(t) = v_1 \phi_1^2(t) + v_2 \phi_2^2(t), \quad (2b)$$

$$m_2(t) = v_3 \phi_1(t) \phi_2(t). \quad (2c)$$

For the long-time limit of Eq (2), one gets a parameterized representation of the transition surface [13],

$$v_3^c = x, \quad f_1^c = y. \quad (3a)$$

$$v_1^c = \frac{3 - (2+x)y}{2(1-y)^2 y (2-xy)}, \quad (3b)$$

$$v_2^c = \frac{x^2 y (y^2 - 2y^3)}{2(1-y)^2 (x^2 y^2 - 3xy + 2)}. \quad (3c)$$

The variables x and y with $x > 4$ and $1/2 \leq y \leq 3/(2+x)$ serve as surface parameters. The exponent parameter $\lambda = 1 - \mu_2$ is determined by

$$\mu_2 = \frac{(3x^2 + 6x)y^3 - (x^2 + 18x + 8)y^2 + (6x + 18)y - 6}{(2x^2 + 4x)y^3 - 12xy^2 + (2x + 4)y}. \quad (3d)$$

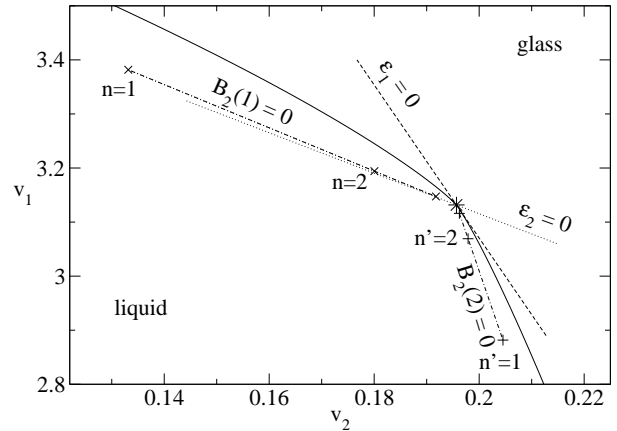


FIGURE 1. Glass-transition diagram for the two-component model for the cut $v_3 = v_3^*$. Liquid-glass transition points are shown by the full line, the A_4 -singularity is shown by a star. The vanishing separation parameters ε_1 and ε_2 are shown by dashed and dotted straight lines, Chain lines mark the location of vanishing correction $B_2(q) = B_2 + K_q B^2$ for $q = 1, 2$ with paths indicated by crosses and pluses, respectively.

The A_3 -singularities are given by $\lambda = 1$ or equivalently $\mu_2 = 0$ in Eq. (3d). For x large enough, such a solution exists with two roots, $y_1(x) < y_2(x)$, where only $y_2(x)$ is relevant. For small x , no such solution exists. Varying x , the two cusp values $y_1(x)$ and $y_2(x)$ coalesce at x^* with $y_1(x^*) = y_2(x^*) = y^*$, defining the A_4 -singularity, $x^* = 24.779392\dots$, $y^* = 0.24266325\dots$.

The cut through the transition surface for $v_3 = x^*$ is shown in Fig. 1 as pair of light full lines joining at the A_4 -singularity which is indicated by a star, $(v_1^*, v_2^*, v_3^*) = (3.132, 0.1957, 24.78)$. Attached to the A_4 -singularity we find the lines of vanishing separation parameters, $\varepsilon_1(\mathbf{V}) = 0$ (dashed) and $\varepsilon_2(\mathbf{V}) = 0$ (dotted), which represent a local coordinate system. The correction amplitudes at the A_4 -singularity are $K_1 = 0.3244$ and $K_2 = -2.109$; these yield two lines of vanishing quadratic correction shown by the chain lines in Fig. 1.

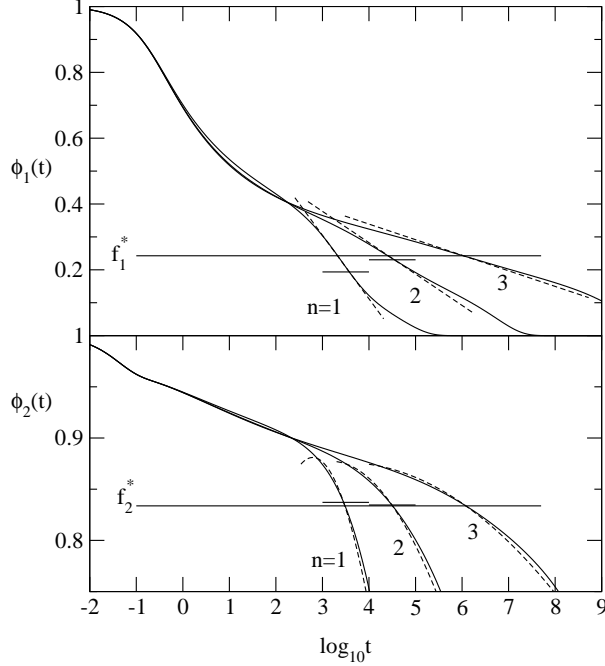


FIGURE 2. Logarithmic decay at the A_4 -singularity on the path (\times) with $n = 1, 2, 3$ in Fig. 1 with $v_1 - v_1^* = 1/2^{n+1}$, $v_2^* - v_2 = 0.25009/2^{n+1}$. The solutions of Eq. (2) are shown as full lines, the approximation (1) as dashed lines. Long horizontal lines exhibit the critical plateau values f_q^* , short lines the corrected plateau values $f_q^* + \hat{f}_q$.

ASYMPTOTIC APPROXIMATIONS

We first analyze the path labeled n (\times) in Fig. 1. The solutions of Eq. (2) are shown as full curves in Fig. 2. The approximations (1) for the correlators are displayed as dashed lines. The time scale τ was matched for $\phi_1(t)$ and $\phi_2(t)$ independently at the corrected plateau values. The approximation describes the decay around the plateaus f_q^* reasonably for both correlators. Since $B_2 + K_1 B^2$ is set to zero on the present path and $B_3 = B_4 = 0$ for an A_4 -singularity [13], only the first line in Eq. (1) is relevant for the upper panel. This approximation describes the decay of $\phi_1(t)$ from 0.4 down to 0.1 and for a win-

dow increasing window in time with increasing n . Since $K_2 < K_1$, the prefactor for the quadratic correction in Eq. (1) for $\phi_2(t)$ is negative and hence the decay around the plateau f_2^* is concave which is described well by the asymptotic approximation. However, for both q the prefactor $(B - B_1)$ slightly overestimates the absolute slope of the solutions. This is due to a relatively large positive next-to-leading-order correction C_1 that renormalizes the prefactor to $(B - B_1 - C_1)$ [26].

Another feature of the curves in Fig. 2 is noteworthy. There appears a window in time outside the transient dynamics between $t \approx 1$ and $t \approx 10^3$ where the description by Eq. (1) is not applicable. This is caused by the close-by A_2 -singularities on the chosen path, cf. Fig. 1, where $f_q^c > f_q^*$, $q = 1, 2$ which introduces an additional slowing down of the dynamics before the logarithmic decay is encountered. In addition, we observe that $\phi_2(t)$ varies almost linearly in $\ln t$ between $t \approx 1$ and $t \approx 250$. It is, however, easy to distinguish that effective logarithmic variation, that stays the same upon further approaching the singularity, from the characteristic behavior of the correlators around the plateau where the prefactor of the logarithmic decay vanishes with the square root of the distance. The almost linear relaxation in $\log t$ seen for $\phi_2(t)$ is related to the β -peak phenomenon [27].

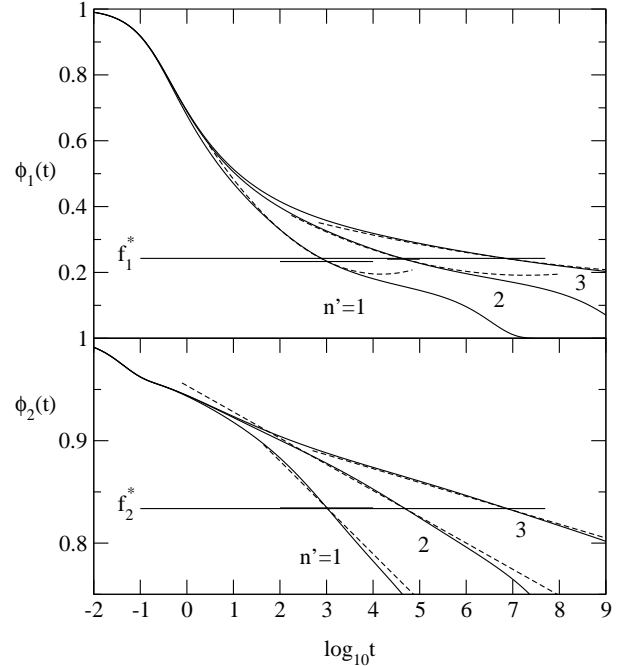


FIGURE 3. Logarithmic decay on the path ($+$) for $n' = 1, 2, 3$ in Fig. 1. $v_1^* - v_1 = 1/4^n$, $v_2 - v_2^* = 0.3541/4^n$. Line styles and notation are the same as in Fig. 2.

In Fig. 3 the quadratic corrections in Eq. (1) for the correlator $\phi_2(t)$ are zero up to higher orders. The quadratic corrections to the first correlator are positive, $B_2(1) > 0$, and $\phi_1(t)$ is convex in $\ln t$ around f_1^* . There

are close-by A_2 -singularities on the chosen path with $f_q^c < f_q^*$, $q = 1, 2$, causing a decay which is encountered after the logarithmic decay, which is seen best for curves $n' = 1$ and $n' = 2$ in the upper panel of Fig. 3 for $\phi_1(t) < 0.15$. While in Fig. 2 the validity of the asymptotic approximation around f_q^* was limited by a higher plateau from above, in Fig. 3 the lower plateaus present a boundary for the application of Eq. (1) from below. Because higher plateaus do not interfere, the asymptotic description applies three decades earlier in Fig. 3 than in Fig. 2 for comparable distances from the A_4 -singularity.

The estimate for the sign of C_1 given above mainly depends on the relative distance of the path chosen in control-parameter space to the lines $\varepsilon_1 = 0$ and $\varepsilon_2 = 0$. As the ordering of the latter two lines and the path is reversed for the case $B_2(2) = 0$ in Fig. 1, C_1 is expected to be negative there. The path labeled n' in Fig. 1 is now closer to the line $\varepsilon_1 = 0$ than to $\varepsilon_2 = 0$. In Fig. 3 we find indeed, that a comparison of solutions and approximations (1) indicates a negative value for C_1 to account for a steeper slope ($B - B_1 - C_1$). Despite those small deviation, the correlators are described well by the asymptotic laws.

The comparison of Figs. 2 and 3 is summarized as follows. For each value of q there exists a line with vanishing quadratic correction $B_2(q)$ for the specified q in the approximation of Eq. (1). On this line, the logarithmic decay is displayed best for the correlator specified by q . Moving to control parameter values above this line, $B_2(q) < 0$, introduces concave decay of the correlator $\phi_q(t)$ in $\ln t$. Going below the line, $B_2(q) > 0$, yields a convex decay in the correlator $\phi_q(t)$. For increasing the value of K_q , the curves specified by $B_2(q) = 0$ rotate clockwise around the A_4 -singularity.

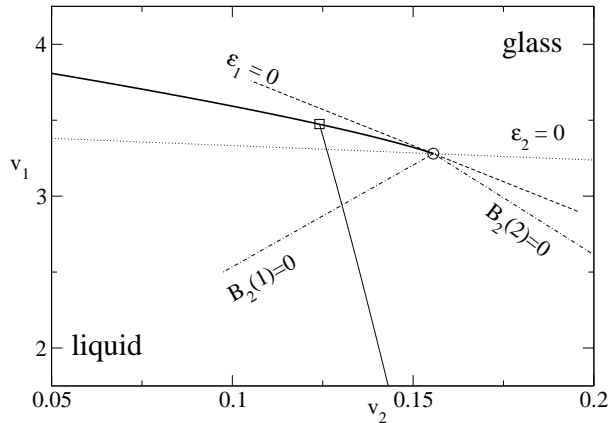


FIGURE 4. Glass-transition diagram for the two-component model for $v_3 = 45$. Notation and line styles are the same as in Fig. 1. The circle marks the A_3 -singularity. Heavy and light full lines denote A_2 -transition points with their respective f_q^c higher and lower than the value f_q^* at the A_3 -singularity. The crossing point of the two lines is indicated by a square.

For control-parameter values $v_3 > v_3^*$, the A_4 -singularity is replaced by an A_3 -singularity which terminates a glass-glass-transition line that extends further into the arrested region as v_3 increases. The lines $\varepsilon_1 = 0$, $\varepsilon_2 = 0$, $B_2(1) = 0$, and $B_2(2) = 0$ for the A_3 -singularities emerge from smooth transformations of the ones at the A_4 -singularity. Figure 4 shows a cut through the transition diagram for $v_3 = 45$. Different from the situation in Fig. 1, the line $B_2(1) = 0$ is now well separated from liquid-glass-transition lines while the line $B_2(2) = 0$ is located completely in the arrested regime. The dynamics on the line $B_2(1) = 0$ for this A_3 -singularity and the related crossing scenario on the same line is discussed in Ref. [13] in great detail.

TIME SCALE

It is obvious from Figs. 2 and 3 that the time scales τ for a given state determined by matching, e.g., $\phi_1(t)$ at f_1^* or $f_1^* + \hat{f}_1$ can deviate considerably. The resulting scale is also different if τ is fixed for different correlators. However, asymptotically close to the higher-order singularity, \hat{f}_q approaches zero and also the time scales determined by using different correlators converge towards each other as explained earlier [13]. Therefore, only the scale fixed by $\phi_1(\tau) = f_1^*$ shall be considered in the following.

The time scale τ when considering only the leading order result in Eq. (1) is given by [28]

$$\log_{10} \tau \propto 1/|\varepsilon_1|^{1/6} \quad (4a)$$

for the A_3 -singularity and from a similar argument [29] for the A_4 -singularity as

$$\log_{10} \tau \propto 1/|\varepsilon_1|^{1/4}. \quad (4b)$$

Thus, the logarithm of the time scale is the relevant quantity to be discussed further on, and $\log_{10} \tau$ is expected to diverge like a power law when the separation from the singularity vanishes. Figure 5 shows that this divergence is indeed stronger for the A_4 -singularity than for the A_3 -singularity. For $|\varepsilon_1| < 10^{-3}$ the time scale τ is described qualitatively by the asymptotic laws. The laws in Eq. (4) were verified quantitatively by extending the analysis to times as large as $\log_{10} \tau \approx 100$. With one exception, the time scales deviate to lower values for τ for larger separations $|\varepsilon_1|$. Hence, the slope of the $\log_{10} \tau$ -versus- $\log_{10}(-\varepsilon_1)$ curve is even larger in that regime than given by the asymptotic laws in Eq. (4). In the lower panel for $|\varepsilon_1| > 10^{-3}$, the time scales for the A_3 -singularity are described better by the law for the close-by A_4 -singularity.

It is seen for the case of the A_4 -singularity that the proximity of a line of liquid-glass transitions (scales τ

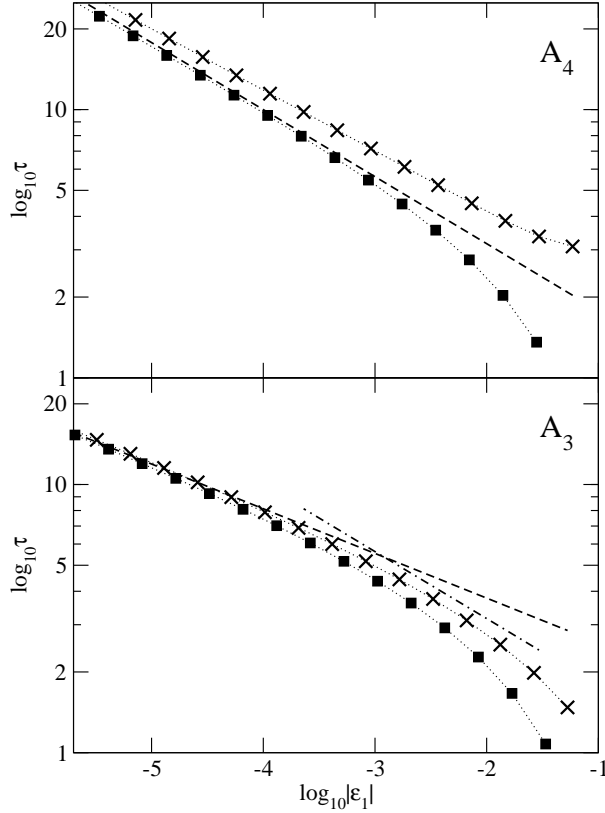


FIGURE 5. Time scale τ determined by matching $\phi_1(t)$ at f_1^* or f_1° for the paths $B_2(1) = 0$ (crosses) and $B_2(2) = 0$ (squares) from Figs. 1 and 4, respectively. The dotted lines are guides to the eye. The corresponding asymptotic laws (dashed lines), $\tau \propto \exp[1/|\epsilon_1|^{1/4}]$ for the A_4 and $\tau \propto \exp[1/|\epsilon_1|^{1/6}]$ for the A_3 are fitted to the data for the paths where $B_2(1) = 0$ around $\tau \approx 10^{100}$. The asymptotic law for the A_4 -singularity is redrawn in the lower panel as chain line.

indicated by crosses) influences also the validity of the asymptotic law for τ : Only for extremely large times, τ follows the law (4b). The time scales are also much larger on that path as discussed already in connection with Fig. 2.

CONCLUSION

It was shown that the asymptotic expansion in Eq. (1) provides a way to divide the control-parameter space into distinct regions by setting the dominant correction to the logarithmic decay laws to zero for different correlators. If plotted in the form of Figs. 1 and 4, the glass-transition diagrams of the two-component model are easily seen to be topologically equivalent to the ones shown for the square-well system in Refs. [14, 17]. For increasing K_q in Eq. (1), the lines of vanishing quadratic corrections

rotate clockwise around the higher-order singularity in the two-component model, which mimics the behavior in the microscopic model for increasing wave vector.

Using the asymptotic expansion to describe the solutions of the equations of motion (2), the approximations fit rather accurately already in a regime that should be accessible to experiments and molecular-dynamics simulations. However, the presence of other glass-transition singularities in the vicinity of higher-order singularities can have drastic influence on the window in time where the logarithmic laws are applicable, cf. Figs. 2 and 3. The validity of Eq. (1) for $\phi_q(t)$ around f_q^* can be bound either from above at earlier times, cf. Fig. 2, or from below to later times, Fig. 3, depending on the specific location of the chosen path in the transition diagram.

The time scale τ asymptotically follows the Vogel-Fulcher-type law of Eq. (4). That the relaxation processes close to higher-order glass-transition singularities are extremely slow is manifested by the fact, that instead of τ itself, the logarithm of the time scale is the relevant quantity that diverges in some power law. The different behavior of τ for A_4 - and A_3 -singularities is clearly seen in the numerical solution of the MCT equations, cf. Fig. 5. However, these asymptotic laws only show up for extremely long times and small distances from the singularity. In addition, other close-by glass-transition singularities can significantly modify the validity of the asymptotic law especially for further separation from the higher-order singularity under consideration.

ACKNOWLEDGMENTS

Fruitful discussion with W. Götze is gratefully acknowledged. This work was supported by the Deutsche Forschungsgemeinschaft Grant No. Go154/13-2.

REFERENCES

1. Bengtzelius, U., Götze, W., and Sjölander, A., *J. Phys. C*, **17**, 5915–5934 (1984).
2. Franosch, T., Fuchs, M., Götze, W., Mayr, M. R., and Singh, A. P., *Phys. Rev. E*, **55**, 7153–7176 (1997).
3. van Megen, W., *Transp. Theory Stat. Phys.*, **24**, 1017–1051 (1995).
4. Kob, W., “Supercooled liquids, the glass transition, and computer simulations,” in *Slow Relaxations and Nonequilibrium Dynamics in Condensed Matter*, edited by J.-L. Barrat, M. Feigelman, J. Kurchan, and J. Dalibard, Springer, Berlin, 2003, vol. Session LXXVII (2002) of *Les Houches Summer Schools of Theoretical Physics*, pp. 199–269.
5. Götze, W., and Haussmann, R., *Z. Phys. B*, **72**, 403–412 (1988).
6. Götze, W., and Sjögren, L., *J. Math. Analysis and Appl.*, **195**, 230–250 (1995).

7. Arnol'd, V. I., *Catastrophe Theory*, Springer, Berlin, 1992, 3rd edn.
8. Fuchs, M., Götze, W., and Mayr, M. R., *Phys. Rev. E*, **58**, 3384–3399 (1998).
9. Götze, W., and Mayr, M. R., “The dynamics of a hard sphere moving in a hard-sphere system near the liquid-glass transition point,” in *Slow Dynamics in Complex Systems*, edited by M. Tokuyama and I. Oppenheim, AIP, New York, 1999, vol. 469 of *AIP Conference Proceedings*, pp. 358–378.
10. Fabbian, L., Götze, W., Sciortino, F., Tartaglia, P., and Thiery, F., *Phys. Rev. E*, **59**, R1347–R1350 (1999).
11. Bergenholtz, J., and Fuchs, M., *Phys. Rev. E*, **59**, 5706–5715 (1999).
12. Dawson, K., Foffi, G., Fuchs, M., Götze, W., Sciortino, F., Sperl, M., Tartaglia, P., Voigtmann, T., and Zaccarelli, E., *Phys. Rev. E*, **63**, 011401 (2001).
13. Götze, W., and Sperl, M., *Phys. Rev. E*, **66**, 011405 (2002).
14. Sperl, M., *Phys. Rev. E*, **68**, 031405 (2003).
15. Puertas, A. M., Fuchs, M., and Cates, M. E., *Phys. Rev. Lett.*, **88**, 098301 (2002).
16. Sciortino, F., Tartaglia, P., and Zaccarelli, E., cond-mat/0304192.
17. Sperl, M., *Phys. Rev. E*, in press (2003), cond-mat/0308425.
18. Mallamace, F., Gambadauro, P., Micali, N., Tartaglia, P., Liao, C., and Chen, S.-H., *Phys. Rev. Lett.*, **84**, 5431–5434 (2000).
19. Pham, K. N., Puertas, A. M., Bergenholtz, J., Egelhaaf, S. U., Moussaïd, A., Pusey, P. N., Schofield, A. B., Cates, M. E., Fuchs, M., and Poon, W. C. K., *Science*, **296**, 104–106 (2002).
20. Chen, W.-R., Chen, S.-H., and Mallamace, F., *Phys. Rev. E*, **66**, 021403 (2002).
21. Poon, W. C. K., Pham, K. N., Egelhaaf, S. U., and Pusey, P. N., *J. Phys.: Condens. Matter*, **16**, S269–S275 (2003).
22. Chen, S.-H., Chen, W.-R., and Mallamace, F., *Science*, **300**, 619–622 (2003).
23. Pham, K. N., Egelhaaf, S. U., Pusey, P. N., and Poon, W. C. K., *Phys. Rev. E*, p. in print (2003).
24. Zaccarelli, E., Foffi, G., Dawson, K. A., Buldyrev, S. V., Sciortino, F., and Tartaglia, P., *Phys. Rev. E*, **66**, 041402 (2002).
25. Bosse, J., and Krieger, U., *J. Phys. C*, **19**, L609–L613 (1987).
26. Sperl, M., *Asymptotic Laws near Higher-Order Glass-Transition Singularities*, Ph.D. thesis, TU München (2003).
27. Götze, W., and Sperl, M., in preparation.
28. Götze, W., and Sjögren, L., *J. Phys.: Condens. Matter*, **1**, 4203–4222 (1989).
29. Flach, S., Götze, W., and Sjögren, L., *Z. Phys. B*, **87**, 29–42 (1992).